Sexual Dimorphism and Retinal Mosaic Diversification following the Evolution of a Violet Receptor in Butterflies

Kyle J. McCulloch,*[,1] Furong Yuan,[1] Ying Zhen,[2] Matthew L. Aardema,[2,3] Gilbert Smith,[1,4] Jorge Llorente-Bousquets,[5] Peter Andolfatto,[2,6] and Adriana D. Briscoe*[,1]

[1]Department of Ecology and Evolutionary Biology, University of California, Irvine, CA

[2]Department of Ecology and Evolutionary Biology, Princeton University, Princeton, NJ

[3]Sackler Institute for Comparative Genomics, American Museum of Natural History, New York, NY

[4]School of Biological Sciences, Bangor University Brambell Laboratories, Bangor Gwynedd, UK

[5]Museo de Zoología, Departamento de Biología Evolutiva, Facultad de Ciencias, Universidad Nacional Autónoma de México, México, D.F., México

[6]The Lewis-Sigler Institute for Integrative Genomics, Princeton University, Princeton, NJ

***Corresponding authors:** E-mails: abriscoe@uci.edu; mccullok@uci.edu.

Associate editor: Patricia Wittkopp

Abstract

Numerous animal lineages have expanded and diversified the opsin-based photoreceptors in their eyes underlying color vision behavior. However, the selective pressures giving rise to new photoreceptors and their spectral tuning remain mostly obscure. Previously, we identified a violet receptor (UV2) that is the result of a UV opsin gene duplication specific to *Heliconius* butterflies. At the same time the violet receptor evolved, *Heliconius* evolved UV-yellow coloration on their wings, due to the pigment 3-hydroxykynurenine (3-OHK) and the nanostructure architecture of the scale cells. In order to better understand the selective pressures giving rise to the violet receptor, we characterized opsin expression patterns using immunostaining (14 species) and RNA-Seq (18 species), and reconstructed evolutionary histories of visual traits in five major lineages within *Heliconius* and one species from the genus *Eueides*. Opsin expression patterns are hyperdiverse within *Heliconius*. We identified six unique retinal mosaics and three distinct forms of sexual dimorphism based on ommatidial types within the genus *Heliconius*. Additionally, phylogenetic analysis revealed independent losses of opsin expression, pseudogenization events, and relaxation of selection on *UVRh2* in one lineage. Despite this diversity, the newly evolved violet receptor is retained across most species and sexes surveyed. Discriminability modeling of behaviorally preferred 3-OHK yellow wing coloration suggests that the violet receptor may facilitate *Heliconius* color vision in the context of conspecific recognition. Our observations give insights into the selective pressures underlying the origins of new visual receptors.

Key words: **butterflies, color vision, photoreceptor cells, short-wavelength opsin, gene duplication, pseudogenes.**

Article

Introduction

How animal eyes have evolved to handle the variety of colorful stimuli they encounter in their world is a key question in visual ecology. Across the animal kingdom, the number of opsin-based photoreceptors used by different species for vision is highly variable. Some insects like honeybees have eyes containing only three opsin-based photoreceptors (Wakakuwa et al. 2005; see Friedrich et al. 2011 for an overview). Other animals have evolved a greatly expanded photoreceptor set, mediated by opsin duplication, expression differences, and filtering effects in the eye. For instance, mantis shrimp have at least 16 spectrally distinct photoreceptors, which they have achieved through multiple opsin gene duplications as well as complex patterns of filtering in the eye (Cronin and Marshall 1989; Cronin et al. 2014; Bok et al. 2015). African cichlid fishes have seven ancestrally duplicated opsin genes, and across the cichlid family the subset of these opsins that are expressed in the photoreceptors of a given species is variable. Diversity in cichlid spectral classes of photoreceptors is also produced by expression level differences (O'Quin et al. 2012; Schulte et al. 2014), coexpression of opsins (Dalton et al. 2017), and by structural changes in the opsin gene (Parry et al. 2005; Seehausen et al. 2008; Hofmann and Carleton 2009; Dalton et al. 2015). Another example is dragonflies which express up to 30 opsin mRNA transcripts, a number that varies between families within the order, although it is not yet known in which photoreceptor cells these opsins are expressed (Futahashi et al. 2015)

The family Papilionidae alone contains species with eight (*Papilio xuthus*) (Koshitaka et al. 2008), nine (*Troides aecus*) (Chen et al. 2013), and 15 (*Graphium sarpedon*) (Chen et al. 2016) spectral classes of photoreceptor. Other groups of butterflies, notably those in the family Nymphalidae, get by with three opsins (Briscoe et al. 2003; Macias-Muñoz et al. 2016), and some even lack the heterogeneously expressed filtering pigments that expand the number of long wavelength-

sensitive photoreceptors found in other butterflies (Briscoe and Bernard 2005). Thus, butterflies rival the mantis shrimp in sheer number of spectral types of photoreceptor but some butterfly species are more like bees, with only three types. However, even among the relatively well-studied butterflies, visual system comparisons between closely related species are rare (although see Frentiu et al. 2007a; Chen et al. 2016). Also, while high levels of photoreceptor spectral diversity have been observed across animal families such as Papilionidae, far less is known about diversification of eyes between closely related species. Given the importance of the social use of color in animals, especially butterflies, it would be surprising if photoreceptor spectral diversification did not play some role in speciation. Yet we know little about the first steps in eye evolution immediately following the fixation of duplicate opsin genes.

Moreover, while numerous kinds of photoreceptors have been discovered in different organisms, the benefits to evolving a new spectral type of photoreceptor and a visual system making use of it are less well understood. Here we begin to close this gap in our knowledge of visual system evolution by conducting an extensive investigation of the retinal mosaics and opsin sequence evolution of *Heliconius* species in comparison to outgroup species in the genus *Eueides*. Famous for their spectacular wing color pattern evolution and mimicry, *Heliconius* butterflies are also interesting for their eyes (Reed et al. 2011; Martin et al. 2012; Nadeau et al. 2016). Other nymphalid butterflies like the monarch butterfly *Danaus plexippus* or the painted lady *Vanessa cardui* have eyes that express three opsins which together with the chromophore 11-*cis*-3-hydroxyretinal encode ultraviolet (UV)-, blue (B)-, and long wavelength (LW)-sensitive rhodopsins (Briscoe et al. 2003; Sauman et al. 2005). *Heliconius* by contrast also express a duplicated ultraviolet (UV) opsin. The gene duplication producing *UVRh1* and *UVRh2* has been identified in all *Heliconius* species so far investigated, together with a 3-hydroxykynurenine (3-OHK) pigment producing UV-yellow coloration on their wings; both traits are shared derived characters of the genus (see below). Evidence for positive selection of *UVRh2* along the branch leading to *Heliconius* suggested it acquired a new adaptive function; specifically, the location of positively selected codons in the chromophore-binding pocket of the rhodopsin implied its wavelength of peak absorbance had shifted (Briscoe et al. 2010). The UV1 opsin, on the other hand, retained an amino acid motif found in sexually monomorphic outgroup taxa lacking the duplicate *UVRh2* gene.

Recently, we determined photoreceptor cell sensitivity and opsin spatial expression patterns in the eye of *Heliconius erato* and found a new spectral function for UV2, as well as maintenance of an older spectral function for UV1 (McCulloch et al. 2016a, 2016b). We found that the UV1 opsin encodes a UV-sensitive rhodopsin with a peak spectral sensitivity or $\lambda_{max} = 355$ nm, similar to the UV-sensitive rhodopsin of other nymphalids (~355 nm, *Vanessa cardui*; ~340 nm *Danaus plexippus*). The UV2 opsin, by contrast, produces a violet-sensitive rhodopsin with a peak sensitivity or $\lambda_{max} = 390$ nm. We were completely surprised to then discover that the *H. erato* eye is sexually dimorphic; each sex possesses a distinct set of ommatidial types based on short-wavelength opsin expression (fig. 1*A*–*D*). By contrast, other investigated nymphalid butterflies such as *Danaus plexippus*, *Limenitis arthemis astyanax* and *Vanessa cardui* have sexually monomorphic eyes (Briscoe et al. 2003; Sauman et al. 2005; Frentiu et al. 2015). Female *H. erato* have UV1, UV2, blue (B), and long wavelength (L) rhodopsin-expressing cells with peak sensitivities at 355, 390, 470, and 555 nm, respectively. Males have the same opsins and sensitivities except they lack a UV1-expressing photoreceptor cell (McCulloch et al. 2016a). The complete absence of one class of opsin in one sex is a new form of sexual dimorphism. Among butterflies with known visual system sex differences, opsin mRNA expression levels are sexually dimorphic in the dry season forms of the nymphalid *Bicyclus anynana* (Everett et al. 2012). Male and female pierids have the same opsin spatial expression patterns, whereas spectral sensitivity is tuned by sexually dimorphic spatial expression of filter pigments (Arikawa et al. 2005; Ogawa et al. 2012, 2013). In some lycaenid butterflies, sex differences are achieved by coexpression of two opsins in the photoreceptor cells of a female-specific ommatidial type (Sison-Mangus et al. 2006).

In light of the rapidly evolving wing signals within and between species in the genus *Heliconius* (for examples of wing color pattern variation in *H. erato* and *H. melpomene* see Van Belleghem et al. 2017 and *Heliconius* Genome Consortium 2012) and the novel pattern of UV opsin expression found in *H. erato*, we thought that *Heliconius* would be a good candidate for investigating how eye evolution and speciation might relate to one another. Other *Heliconius* species have two *UVRh* genes but it is unknown whether they have the same opsin expression as *H. erato* or if their eyes have diverged during speciation. We therefore characterized opsin expression patterns, relative cell abundances, and evolutionary histories of visual traits in species representing five major lineages within *Heliconius* (*erato*, *sara*, silvaniform, *melpomene*, and *doris* clades) and one species from the sister genus *Eueides*. We also used RNA-Seq data to identify changes in the intensity of selection on the opsins. We uncovered widespread diversity between clades together with different forms of sexual dimorphism. These results suggest varying levels of natural and sexual selection have shaped the *Heliconius* eye during speciation.

Results and Discussion

Diverse Opsin Protein and mRNA Expression among *Heliconius* Species

Following the fixation of duplicate genes, one scenario of early events is that males and females would each make use of both copies. Under this scenario, we might expect that after the ancestral UV opsin gene duplicated, both *Heliconius* sexes expressed UV1 and UV2 opsins. To better understand the origins of the violet receptor (UV2) and how it came to replace the ultraviolet receptor (UV1) in the male *H. erato* eye, we first asked whether the observed sexual dimorphism (McCulloch et al. 2016a) is found throughout the genus, or whether there are *Heliconius* species in which both UV1 and

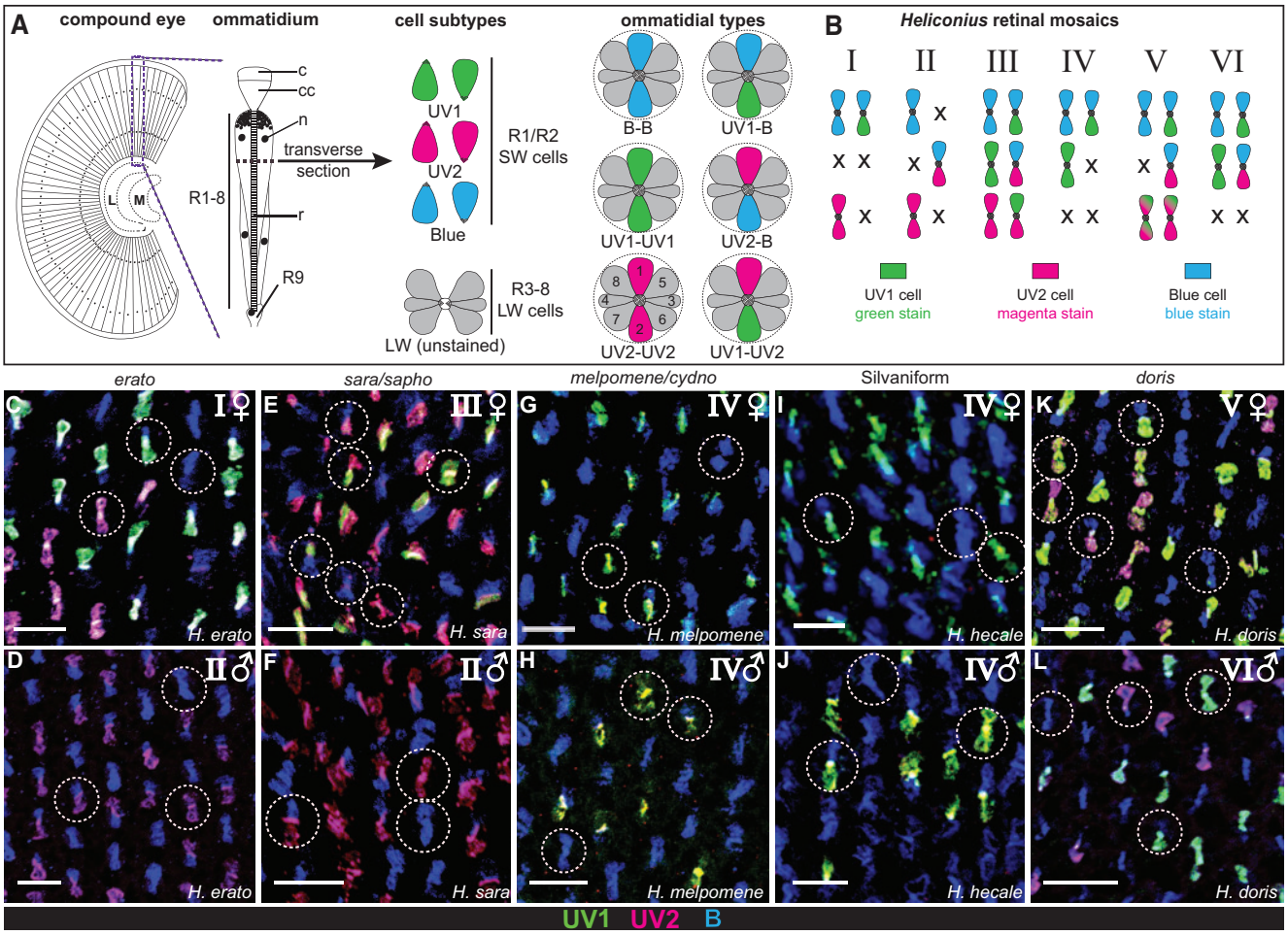

Fig. 1. At least six retinal mosaics are found in *Heliconius*. (*A*) From left to right: schematic of the compound eye, longitudinal section of a single ommatidium, individual photoreceptor cell subtypes, and total number of ommatidial types showing variable short wavelength (SW) opsin expression in the main retina across surveyed *Heliconius* species. R1 and R2 photoreceptor cells express blue (blue), UV1 (green), or UV2 (magenta) opsins. Magenta and green stripes indicate that *Heliconius doris* females coexpress UV1 and UV2 opsins in some R1 and R2 cells. R3–8 cells express long wavelength (LW) opsin. L, lamina; M, medulla c, cornea; cc, crystalline cone; n, nucleus; r, rhabdom. (*B*) Retinal mosaics are identified based on patterns of SW opsin expression and numbered I–VI. (*C*–*L*) Female and male transverse sections of *Heliconius* compound eyes, representing each major clade in the genus. Roman numerals in each panel indicate the retinal mosaic for each species and sex. (*C* and *D*) *H. erato*, (*E* and *F*) *H. sara*, (*G* and *H*) *H. melpomene*, (*I* and *J*) *H. hecale*, and (*K* and *L*) *H. doris*. Circles highlight distinct ommatidial types identified within each eye. Scale bars, 25 μm.

UV2 opsins are expressed in both sexes. We used antibodies against the short-wavelength opsins (UV1, UV2, and B) to immunostain transverse sections of ommatidia in the compound eyes of males and females of 13 species in five major clades within *Heliconius* and one outgroup in the genus *Eueides*. R1 and R2 photoreceptor cell subtypes express short wavelength (SW) opsins in different combinations (fig. 1*A*). We discovered that the sexual dimorphism in *H. erato* is not conserved across the genus. In fact, there are at least six distinct retinal mosaics in *Heliconius* based on the different combinations of SW opsins present in the eye, with all but one incorporating the more recently derived violet-sensitive rhodopsin UV2 (fig. 1*B*–*L*).

For the 14 species examined, each sex within a clade shares the same retinal mosaic except for *H. charithonia* (see below); however, retinal mosaics differ considerably between clades and sexes. Other *erato* clade members (two species) have the same expression pattern as *H. erato*, where UV1 opsin expression is absent in the male eye and UV2 is present in both sexes (females, mosaic I; males, mosaic II, fig. 1*C* and *D*, supplementary fig. S1*A*–*C*, Supplementary Material online; McCulloch et al. 2016a). A second form of sexual dimorphism is found in the *sara* clade (five species, supplementary fig. S1*D*–*H*, Supplementary Material online). Unlike *H. erato*, females in this clade express at least six ommatidial types based on SW opsin expression (mosaic III, fig. 1*E*), whereas *sara* males resemble *H. erato* males (mosaic II, fig. 1*D* and *F*). The *melpomene* (two species) and silvaniform (two species) sister clades exhibit yet another retinal mosaic. In this clade, neither sex expresses the UV2 rhodopsin in the eye, resulting in mosaic IV (fig. 1*G*–*J*, supplementary fig. 1*I*–*L*, Supplementary Material online). *Eueides isabella*, a sister taxon to *Heliconius* lacking the *UVRh2* duplicate, resembles *melpomene* and silvaniform clades with respect to sexually monomorphic UV1 expression (supplementary fig. S1*M*, Supplementary Material online). This expression pattern

together with the sensitivity of the UV1 rhodopsin are similar to other nymphalid butterflies such as *Vanessa cardui* (~355 nm), and *Danaus plexippus* (~340 nm) suggesting maintenance of the ancestral role for this photoreceptor subtype (Briscoe et al. 2003; Stalleicken et al. 2006; Blackiston et al. 2011). A third form of sexual dimorphism is evident in *H. doris*. Both *H. doris* sexes make use of UV1 and UV2 rhodopsins, in mosaic V in females (fig. 1*K*) and mosaic VI in males (fig. 1*L*, supplementary fig. S1*N*, Supplementary Material online).

To complement our protein expression data, we used RNA-Seq to quantify levels of opsin mRNA expression in 18 species ($n = 60$ individual butterflies) (supplementary tables S1 and S2, Supplementary Material online). In the *erato* (four species) and *sara* (five species) clades, *UVRh1* expression is nearly absent in males, whereas *UVRh2* expression is high; females highly express both *UVRh1* and *UVRh2* (supplementary table S2, Supplementary Material online). Both sexes in the *doris* clade (three species) express both *UVRh1* and *UVRh2*, consistent with the *H. doris* opsin immunostaining pattern (supplementary table S2, Supplementary Material online). In agreement with our protein expression data, all *melpomene* and silvaniform species (five species) have low expression of *UVRh2* in both sexes, whereas *UVRh1* remains highly expressed (supplementary table S2, Supplementary Material online). RNA sequencing together with GenBank sequences (Bybee et al. 2012; Yuan et al. 2010) also revealed that *UVRh2* is pseudogenized in several silvaniform species (see below), but not in *H. melpomene*, *H. cydno*, *H. pachinus*, and *H. timareta*.

Evidence for sexually dimorphic patterns of opsin expression as seen in *erato* and *sara* clades is limited in other insects. Sexual dimorphism in other investigated butterflies is accomplished via sex differences in eye filter pigment distribution that causes shifts in photoreceptor sensitivity, or via sex-specific coexpression of opsins in a subset of photoreceptor cells (Arikawa et al. 2005; Sison-Mangus et al. 2006; Ogawa et al. 2012, 2013). Seasonally sexually dimorphic opsin mRNA expression levels are seen in *Bicyclus anynana* (Everett et al. 2012); the moth *Manduca sexta* has sexually dimorphic expression of genes involved in the deactivation of rhodopsin signaling (Smith et al. 2014). In addition to Lepidoptera, known examples of sexual dimorphism in the compound eyes of honeybees and houseflies involve differences in the domain of opsin expression rather than loss of opsin expression in one sex (Franceschini et al. 1981; Menzel et al. 1991). Some evidence for sex differences in *LWRh* expression has been observed in the fig wasp *Ceratosolen solmsi* (Wang et al. 2013), but quantification of mRNA levels alone does not reveal opsin spatial expression, or whether differences in spectral sensitivity exist. Thus, the male-specific loss of the UV1-expressing cell we document in some *Heliconius* lineages represents a newly described form of sexual dimorphism in insects.

Variation in Photoreceptor Cell and Ommatidial Number

If the regulatory mechanisms that control the differentiation of ommatidial types are conserved in *Heliconius*, then we would expect to observe fixed proportions of stochastically distributed ommatidial types shared among species within clades with the same retinal mosaic, whereas these proportions should diverge between clades (Wernet et al. 2015). Similar proportions of ommatidial types in related species is evidence of a single evolutionary origin of changes to retinal mosaic developmental pathways. We therefore calculated average percentages of ommatidial types in multiple individuals for each species and sex ($n = 33{,}449$ ommatidia total). Within each clade, the abundance of each ommatidial type is similar and sex-specific; between clades there are notable differences (supplementary table S3, Supplementary Material online). To visualize the overall pattern of the abundances for each ommatidial type, we plotted the results of a principal component analysis (PCA) using the percentages of ommatidial types from each sex from 14 species (fig. 2). This PCA reveals four distinct clusters (dotted circles, fig. 2) and one outlier, *H. doris*. The clusters suggest a common origin of retinal mosaic II in *sara* and *erato* clade males, and of retinal mosaic IV in *melpomene* and silvaniform clades. *H. doris* males are distinct in that they do not obviously cluster with other clades in the PCA plot. *H. doris* males are the only males that express both UV1 and UV2 rhodopsins (fig. 1*L*). *H. doris* females but not males are also the only individuals where our immunohistochemistry indicates coexpression of UV1 and UV2 rhodopsins in a subset of R1 and R2 photoreceptor cells, so we did not include them in the analysis. Overall, our PCA reveals clade-specific patterns of fixed proportions of ommatidial types, providing evidence for conserved regulatory mechanisms that give rise to these differing retinal mosaics within the genus.

Stochastic spatial expression yet fixed proportions of ommatidial subtypes are found in numerous insects (Arikawa 2003; Wernet et al. 2015). In the *D. melanogaster* retina, stochastic expression of the transcription factor Spineless in R7 photoreceptors leads to stereotypical ratios of two ommatidial types defined by stochastic expression of opsins (Cook et al. 2003; Domingos et al. 2004; Mikeladze-Dvali et al. 2005; Wernet et al. 2006). Recently butterflies were shown to have two cells homologous to the single *D. melanogaster* R7 subtype (Perry et al. 2016). The decision to express either the UV or blue-sensitive rhodopsin in butterfly R1 and R2 color-sensing cells depends on *spineless* expression where two independent stochastic binary decisions produce the three ancestral types of ommatidia seen throughout the Lepidoptera (UV/UV, UV/B, or B/B) (Perry et al. 2016). This mechanism alone cannot account for the additional complexity found in *Heliconius* species that produce mosaic III. It is possible that a second stochastic decision has been added to the process of cell fate specification: initially, *spineless* expression could control the UV versus B decision and then a second stochastic decision may determine whether this cell is a UV1 or UV2 cell. Additional mechanisms would be required for: i) the restriction of ommatidial types observed in *erato* clade females—despite expression of UV1, UV2, and blue cell subtypes—and ii) the suppression of the UV1 cell subtype in *erato* and *sara* clade males in favor of UV2. This should be a rich area for future research on sexual dimorphism in visual system patterning and function.

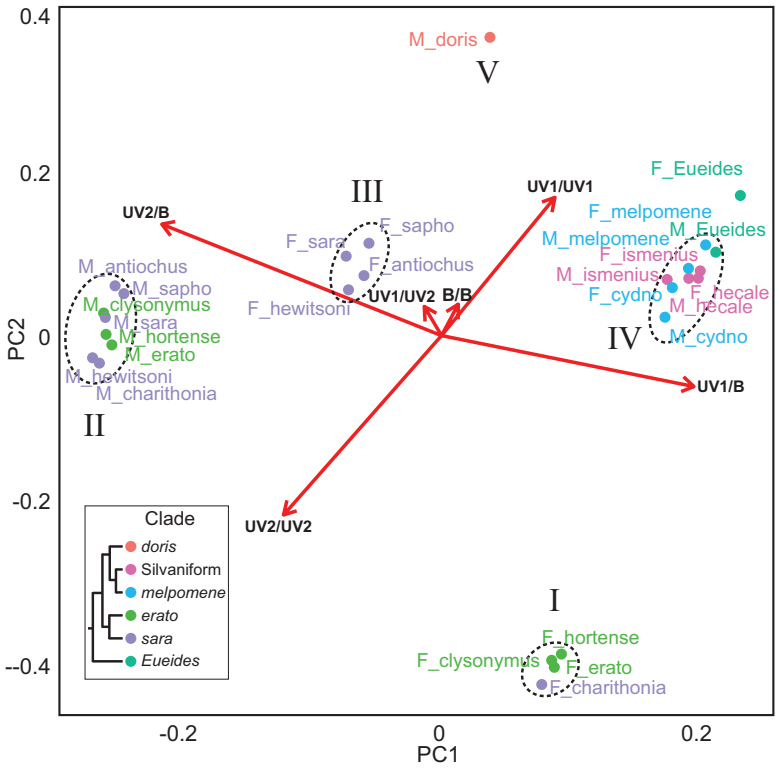

Fig. 2. Principal component analysis showing similar proportions of ommatidial types within clades and divergent proportions between clades by sex. Data is plotted in two dimensions using the first two principal components, totaling 73% of the variance in the analysis. Eigenvectors are shown for this analysis with each vector representing an ommatidial type (red arrows). Averages of ommatidial percentages were used for analysis. Labels list the sex (M, male or F, female) and species for each point, colors correspond to the clade in which the species belongs. Dotted circles indicate clustering of *sara*/*erato* clade males (left), *sara* clade females (center), *melpomene*/silvaniform clades both sexes (right), and *erato* clade/*H. charithonia* females (bottom). Roman numerals correspond to retinal mosaic type.

Relaxation of Selection and Loss of UV2 Rhodopsin Expression

Despite evolving a new violet receptor at the base of the genus *Heliconius*, it appears that UV2 expression has been lost in all *melpomene* and silvaniform species so far investigated and that these species have reverted to an ancestral UV1-expressing retina. In previous work, we identified full-length *UVRh2* mRNAs in *melpomene*-clade species (Briscoe et al. 2010). However *H. melpomene* and *H. cydno* lack a UV2-expressing photoreceptor in the compound eye (fig. 1*G* and *H*, supplementary fig. S1*I* and *J*, Supplementary Material online), and in *H. melpomene* whole heads ($n = 4$) full-length *UVRh2* mRNA is present in low levels (supplementary table S2, Supplementary Material online). This suggests that *UVRh2* may be expressed in the brain in an extraretinal photoreceptor (Lampel et al. 2005). Unlike *H. melpomene*, several silvaniform species have pseudogenized *UVRh2* (fig. 3*A* and *B*, supplementary table S4, Supplementary Material online). Specifically, *H. atthis* and *H. elevatus* have full-length *UVRh2* mRNAs, whereas *H. pardalinus* and *H. ethilla* do not. RNA-Seq shows that *H. numata* and *H. hecale* are polymorphic for full-length and truncated *UVRh2* mRNAs (fig. 3*B*, supplementary table S4, Supplementary Material online). Character mapping of *UVRh2* pseudogenes on a species phylogeny reveals at least four independent loss-of-function events in silvaniform *UVRh2* evolutionary history (fig. 3*B*).

Since *UVRh2* has lost its role in vision in the *melpomene*/silvaniform clades, we expected to observe relaxation of selection on *UVRh2* in these clades. We formally tested this hypothesis using RELAX in HyPhy (Pond et al. 2005) with an expanded opsin data set consisting of sequences from 25 *Heliconius*, five *Eueides*, two *Dione* and one *Agraulis* species ($n = 71$ individuals; supplementary table S1 and fig. S2, Supplementary Material online) (Wertheim et al. 2015). We found a significant difference favoring a model where *melpomene*/silvaniform *UVRh2* genes are evolving under relaxed selection compared with the null model where *melpomene*/silvaniform branches have the same selection pressures as all other *UVRh2* branches (relaxation parameter, $k = 0.6292$; $k = 1$ would mean the test branch is evolving under either purifying or positive selection at the same rate as the reference branches; chi-squared test, $P = 0.001$, fig. 4*A*). The RELAX method builds on a random effects branch-site model (Kosakovsky Pond et al. 2011), and compares the distribution of ω values between the a priori defined reference branches and test branches. When selection is relaxed on the test branches, the sites on the reference branches with ω values undergoing either purifying selection ($\omega < 1$) or positive

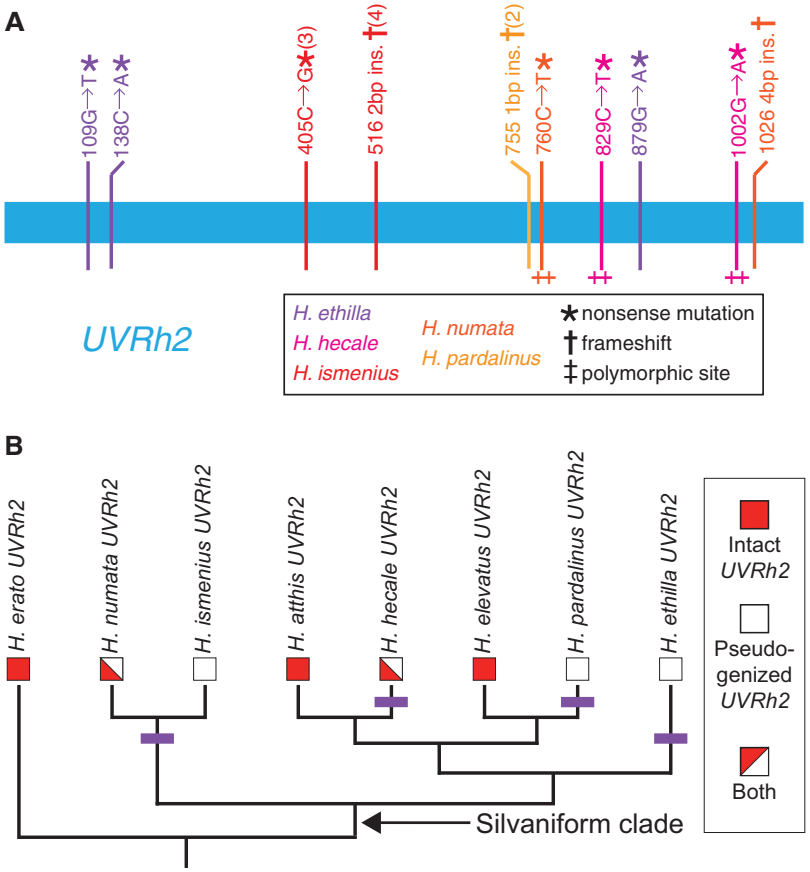

Fig. 3. Parallel loss of *UVRh2* mRNAs in *Heliconius*. (*A*) Schematic of identified silvaniform loss-of-function mutations in *UVRh2*. Color of the mutation corresponds to the species in which it was identified. Symbols indicate the type of mutation. Numbers in parentheses indicate the number of individuals identified with the same mutation. No number indicates only one individual identified with the mutation. Further mutation information for each individual can be found in supplementary table S4, Supplementary Material online. (*B*) Silvaniform species phylogeny with outgroup *H. erato*. Transcripts were either intact (red boxes) or pseudogenized (white boxes). Some individuals were heterozygous (half red, half white). Purple bars indicate loss-of-function mutation events. Phylogeny from Kozak et al. (2015).

selection ($\omega > 1$) will be pushed toward neutrality ($\omega = 1$) on the test branches (fig. 4*B*).

Evolutionary History of the UV2 Opsin and the Evolution of a New Female Retinal Mosaic

To trace the evolution of the UV2 opsin and the UV2-expressing eye of *erato* and *sara*-clade males, we reconstructed ancestral states for several traits (supplementary fig. S3*A*–*F*, Supplementary Material online). Maximum likelihood models indicate that both sexes probably had UV1 and UV2 rhodopsins in the common ancestor of *Heliconius* (supplementary fig. S3*A*–*D*, Supplementary Material online). Down-regulation of *UVRh1* in males appears to have evolved once in the ancestor to the *erato* and *sara* clade (supplementary fig. S3*C*, Supplementary Material online). As the *melpomene*/silvaniform lineage split from the rest of the genus, both sexes lost the UV2 rhodopsin in their compound eyes (supplementary fig. S3*B* and *D*, Supplementary Material online), as noted above. Further relaxation of selection of *UVRh2* resulted in multiple parallel pseudogenizations as the silvaniforms diverged from the *melpomene* clade (figs. 3*A*, *B* and 4, supplementary fig. S3*F*, Supplementary Material online).

Although several *Heliconius* lineages have downregulated or lost the UV2 rhodopsin, other *Heliconius* lineages appear to have undergone sex-specific selection for retinal mosaics expressing UV2. It appears that the female-specific retinal mosaic III expressing both UV1 and UV2 opsins evolved after the split between *H. charithonia* and the lineage leading to the rest of the *sara*/*sapho* clade. The eyes of *H. charithonia* males resemble other *sara* and *erato* clade males (mosaic II, figs. 1*D*, *F* and 5*A*). However females in the *sara* and *erato* clades differ, and *H. charithonia* female eyes have mosaic I, similar to *erato*-clade females, rather than mosaic III as found in other *sara* clade females (fig. 5*B*, supplementary fig. S1*A*–*H*, Supplementary Material online). Evidence for the evolution of a new female retinal mosaic following speciation comes from closer phylogenetic examination of *H. charithonia* in relation to other members of the *sara* clade. In opsin gene phylogenies (266 sequences total), *H. charithonia UVRh1*, *UVRh2*, *BRh*, and *LWRh* opsins each fall within a monophyletic clade together with other *sara* clade opsins (supplementary fig. S2*A*–*C*, Supplementary Material online). Confirming previous phylogenetic analyses (Kozak et al. 2015), a species phylogeny using 634 orthologous genes from whole

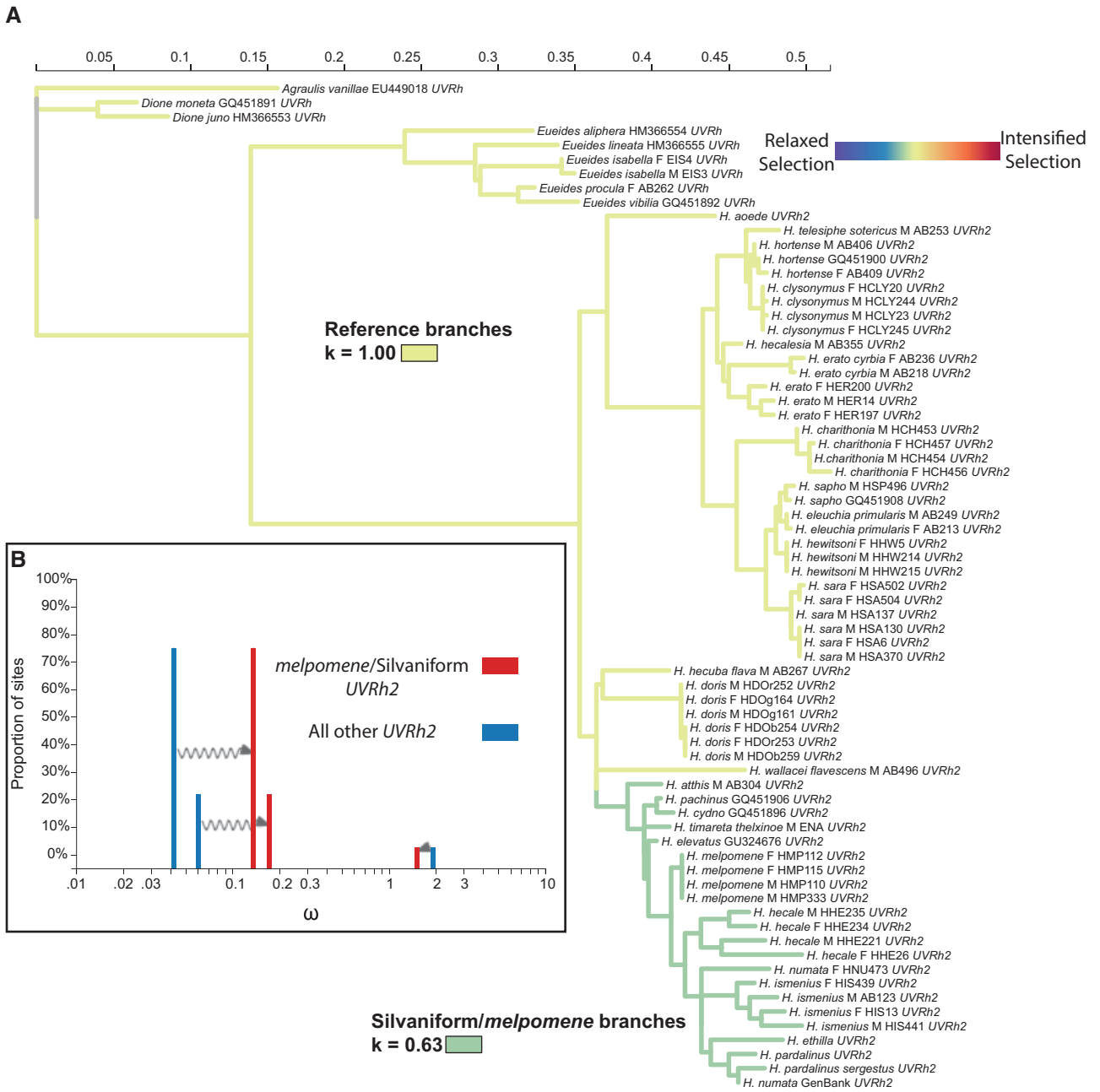

Fig. 4. Selection on *UVRh2* is relaxed in *melpomene*/silvaniform clades. (*A*) Gene tree showing test branches of silvaniform/*melpomene* *UVRh2* (light green) associated with a relaxation parameter, $k < 1$, relative to reference *UVRh* branches (yellow) set at $k = 1$, signifying relaxed selection in the test branches. The legend represents the relative value of the selection parameter, *k*, where cooler colors show relaxed selection and warmer colors show intensified selection. (*B*) Comparison of ω distributions from *melpomene*/silvaniform *UVRh2* branches (red) and all other *UVRh* branches (blue) under the alternative model of relaxed selection. Sites under positive ($\omega > 1$) or purifying ($\omega < 1$) selection in other *UVRh* branches move toward neutrality in the *melpomene*/silvaniform *UVRh2* branches ($\omega = 1$). In the BS-REL model, ω values for each site are binned into three ω distributions corresponding to sites under strong purifying, weakly purifying/nearly neutral, and positive selection. Arrows indicate that when comparing sites in the reference branches to the corresponding sites in the test branches, all three ω distributions move toward neutrality in the test branches.

transcriptomes of five species, also gives strong support for *H. charithonia*'s inclusion within the *sara* clade (supplementary fig. S4, Supplementary Material online). Beyond the sexual dimorphisms documented above, *H. charithonia* provides further evidence that differential selection pressures may be shaping the male and female *Heliconius* eye.

Discriminability Modeling of 3-OHK Yellow Coloration and a Potential Benefit of the Violet Receptor

The newly evolved UV2-expressing violet receptor appears in the eyes of butterflies in seven *Heliconius* clades ($n = 13$ species, supplementary table S2, Supplementary Material online), and has been lost in the *melpomene* and silvaniform lineages

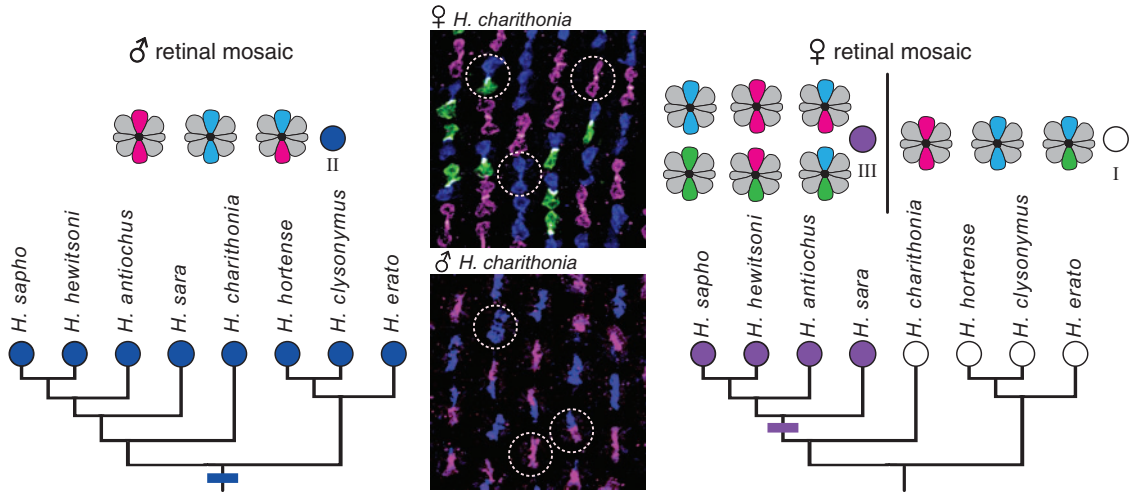

Fig. 5. Male and female *Heliconius charithonia* eyes are evolving under different selection pressures. *sara* and *erato* clade retinal mosaics mapped on to the species phylogeny. (*A*) Males all have the same retinal mosaic (blue circles, II), with the origin of the trait in the ancestor of both clades (blue bar). (*B*) *sara* clade females have retinal mosaic type III (purple circles) except for *H. charithonia*, with retinal mosaic I (white circles). The most parsimonious origin of retinal mosaic III is after *H. charithonia* split from the rest of the *sara* clade (purple bar). Inset shows immunostain of male and female *H. charithonia* with UV1 (green), UV2 (magenta), and blue opsins (blue).

($n = 5$ species, supplementary table S2, Supplementary Material online, see below). What might be the benefit of evolving a new violet receptor and a visual system making use of this receptor? While the violet receptor appears in retinal mosaics with varying numbers of ommatidial types in *Heliconius*, the biggest functional impact on color vision is expected to be due to its spectral tuning. Previously we used linear discriminant analysis to show that a tetrachromatic color vision system similar to the female *H. erato* eye—and ancestral male and female *Heliconius* eyes—consisting of UV, V, B, and L photoreceptors would outperform both avian and butterfly visual systems lacking both duplicated UVs in discriminating *Heliconius* 3-hydroxykynurenine (3-OHK) UV-yellow from other yellow coloration (Bybee et al. 2012). These results suggested that the evolution of the duplicated UVs together with 3-OHK coloration (fig. 6*A* and *B*, yellow lines) at the base of the genus *Heliconius* (fig. 6*C*, arrows)—before subsequent evolution of these diverse retinal mosaics in descent lineages—may have been beneficial for conspecific communication in the context of mimicry. However, these calculations were performed before we knew that male and female *H. erato* eyes were sexually dimorphic and before we had photoreceptor count data for each sex. It is worth reconsidering this argument using a more biologically realistic model, which incorporates these parameters (Vorobyev and Osorio 1998).

To understand the potential benefit of the UV2-expressing eye, we performed *H. erato* male and female mate choice experiments with chromatic stimuli resembling 3-OHK yellows of *Heliconius* and non3-OHK yellows of *Heliconius* comimics from the genus *Eueides* (fig. 6*A* and *B*, grey lines). We found that both *H. erato petiverana* males and females do indeed prefer 3-OHK yellow to non3-OHK yellows (Finkbeiner et al. 2017). To better understand this preference in relationship to male and female *H. erato* visual performance, here we performed pairwise discriminability calculations under high light illumination comparing *H. erato* yellow dorsal wing colors ($n = 14$) to *Eueides* yellows ($n = 11$) for three types of visual system: a real *H. erato* female with UV1, UV2 (V), B, and L photoreceptors (fig. 6*A* and *B*, solid and dotted black lines), a real *H. erato* male with UV2 (V), B and L photoreceptors (fig. 6*A* and *B*, solid black lines) and a hypothetical *H. erato* male with UV1 (fig. 6*A* and *B*, dotted black line), B and L photoreceptors (for both models, Weber fraction = 0.05, (Koshitaka et al. 2008); relative abundances of photoreceptors, UV = 0.09, V = 0.07, B = 0.17, G = 1 (female) or V (or UV) = 0.13, B = 0.2, L = 1 (male), (McCulloch et al. 2016a). We found that the actual male *H. erato* visual system with the adaptively evolving UV2 opsin outperformed a hypothetical male *H. erato* visual system with the ancestral UV1 opsin in discriminating *H. erato* yellows from *Eueides* yellows *and* the female eye with both UV1 and UV2. The number of pairwise comparisons ($n = 144$) that exceeded a threshold of one just noticeable difference (JND), meaning the colors could be discriminated, was 78.4% for the UV2 male eye, 48.6% for the UV1 male eye, and 45.1% for the female eye with both UV1 and UV2 (table 1). All three types of eyes performed similarly when discriminating ventral colors. Taken together, these results suggest that the avoidance of similar-looking but unrelated species in the context of intraspecific communication and mate choice may have been a key driving force for the evolution of the violet receptor. The deployment of a UV-yellow wing pigment for signaling at the base of the genus *Heliconius* helps explain the spectral tuning of the violet-sensitive rhodopsin UV2 and its use in *Heliconius* eyes.

The loss of the UV2 opsin in some *Heliconius* species nonetheless suggests it is evolving neutrally in those lineages due to other genetic and/or environmental changes. Both UV2 opsin down regulation and *UVRh2* pseudogenization in the *melpomene*/silvaniform clades represent recent and ongoing processes. If *melpomene*/silvaniform species retain a

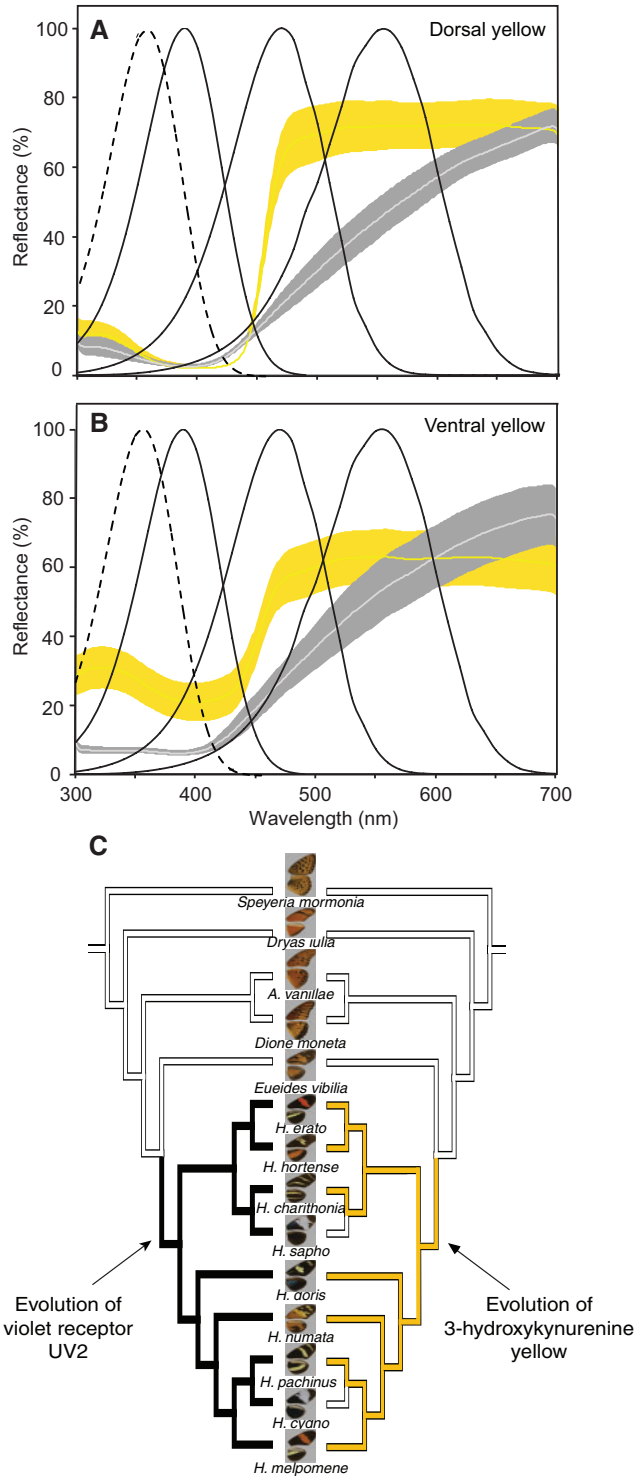

Fig. 6. Reflectance spectra of *H. erato* and *Eueides* yellow wing coloration used in the discriminability analysis. (*A*) Dorsal yellow wing colors and (*B*) Ventral yellow wing colors. Yellow indicates 3-hydroxykynurenine yellow of *Heliconius erato*. Grey indicates *Eueides* yellow. Shaded areas correspond to 95% confidence intervals. Solid yellow or light grey lines are means. Black lines indicate normalized UV2, B, and L photoreceptors' spectral sensitivities from the male *H. erato* eye. Dotted lines indicate normalized UV1 photoreceptor spectral sensitivity of the *H. erato* female eye. Data from McCulloch et al. (2016a, b). (*C*) Phylogeny of Heliconiini species in which presence (black) or absence (white) of the UV2 photoreceptor or presence (yellow) or absence (white) of 3-OHK pigment is mapped. Modified from Briscoe et al. (2010).

Table 1. Percentage of *Heliconius erato* and *Eueides* Dorsal and Ventral Yellow Wing Colors with Chromatic JND Values >1 for Different *H. erato* Visual Systems.

	N	UV1 Male (%)	UV2 Male (%)	UV1 and UV2 Female (%)
Dorsal yellow	**144**	**48.6**	**78.5**	**45.1**
Ventral yellow	**117**	**88.9**	**87.2**	**84.6**

Note.—Three visual systems are modeled: the hypothetical UV1 male, the UV2 male and the UV1 and UV2 female *H. erato* eye under high light, sunny illumination. All visual systems include B and L opsins.

UV1-expressing photoreceptor cell with similar sensitivity as *H. erato* UV1 rhodopsin, these species may be less able to discern variation in UV-yellow wing coloration than species in the *erato/sara/doris* clades, a possibility that would need to be confirmed with electrophysiological recordings and behavioral experiments. Interestingly, rampant hybridization exists between species in the *melpomene* and silvaniform clades. It is conceivable that loss of UV2 in these clades may have contributed to increased hybridization via a reduction in visual ability to recognize conspecifics (Estrada and Jiggins 2008; *Heliconius* Genome Consortium 2012). The multiple instances of pseudogenizing mutations in *UVRh2* suggest that other kinds of cues such as olfaction (Andersson and Dobson 2003; Schulz et al. 2008; Briscoe et al. 2013; van Schooten et al. 2016), may play an increasingly critical role in mate recognition and foraging in species that have lost the duplicate UV opsin.

In summary, we have identified an unprecedented diversity of opsin expression patterns and retinal mosaics among closely related species (fig. 7). Changes in opsin expression have resulted in multiple forms of sexual dimorphism, parallel losses of the *UVRh2* gene, losses of both UV1- and UV2-expressing cells, and imply that differential selection pressures have shaped the male and female eye. Nonetheless most studied *Heliconius* species retain the newly evolved UV2-expressing violet receptor, either alone or with the UV1-expressing ultraviolet receptor, which facilitates discrimination of 3-OHK yellow from other yellow coloration in behavioral tests. Our findings substantiate and elaborate our understanding of the origins and spectral tuning of a new opsin-based violet receptor and its relationship to 3-OHK yellow signaling in *Heliconius*.

Materials and Methods

Animals

We obtained pupae from The Butterfly Farm—Costa Rica Entomological Supply, or from Stratford Butterfly Farm, U.K. After eclosion, butterflies were kept alive for 2–3 days in a humidified chamber and fed a diluted honey solution daily before sacrificing. Other adult butterflies used for mRNA sequencing were collected in the field in Ecuador or México and preserved in RNAlater (Life Technologies, Grand Island, NY). Only one color morph was used per species, except for *H. doris* where all three color morphs were sampled.

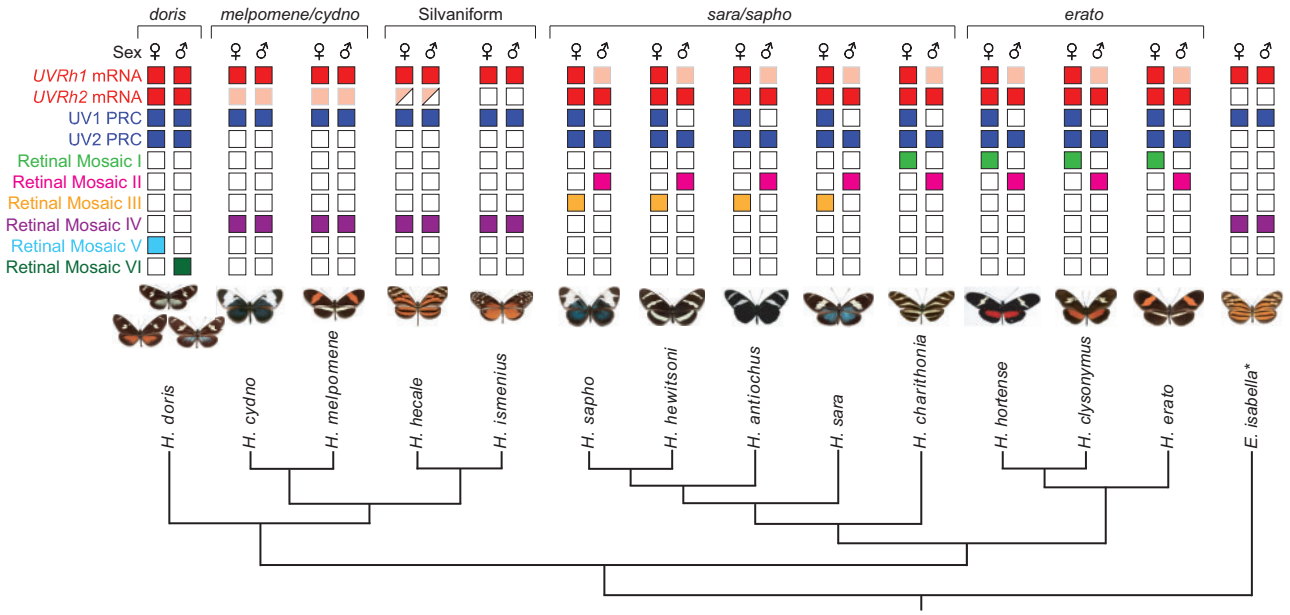

Fig. 7. Summary of UV opsin character states on the *Heliconius* phylogeny. Each trait was scored for presence (filled box) or absence (open box) based on immunohistochemistry of adult eyes and mRNA-Seq of adult heads. Some species are polymorphic for the trait (half-filled boxes). For all species, traits are listed for both sexes. *UVRh1* and *UVRh2* mRNAs (red) signify full-length transcripts for UV1 and UV2 opsins, respectively. Lighter-shaded (pink) boxes indicate low-level mRNA expression. mRNA expression data only for six other species are given in supplementary table S2, Supplementary Material online. Photoreceptor cell subtypes found in either males or females are indicated according to UV1 or UV2 opsin expression (dark blue). Retinal mosaic types I–VI (light green, magenta, orange, purple, light blue, and dark green), characterized by the type of ommatidia expressed in each species and sex, are also mapped on the species phylogeny of (Kozak et al. 2015).

Cryosectioning

Butterfly heads were cut in two to separate the eyes. Both eyes were fixed in 4% paraformaldehyde (Electron Microscopy Sciences Cat. # 15710) in 0.1 M phosphate buffered saline (PBS) for 1 h at room temperature. Eyes were then sucrose-protected in increasing concentrations of 10%, 20%, and 30% sucrose in PBS for either 1 h at room temperature or overnight at 4 °C. Excess cuticle was cut away around each eye before it was placed on a bed of Tissue Tek O.C.T. compound and frozen at −20 °C. Frozen eyes were sectioned at 14 µm thickness on an HM 500 OM microtome cryostat (Microm), and placed on slides to dry overnight at room temperature.

Immunohistochemistry

An antibody against the peptide DGLDSVDLAVIPEH in the N-terminal domain of the *Heliconius erato* UV1 opsin was generated in guinea pigs and immunoaffinity purified (Open Biosystems, Inc., Huntsville, Alabama). This motif is conserved in UV1 in *Heliconius* and in other UV opsins in the tribe Heliconiini (*Eueides*, *Dione*, *Agraulis*, and *Speyeria*) but not in UV2 of *Heliconius*. An antiblue opsin antibody was generated in rats against the *H. erato* peptide RYRAELQKRLPWMGVREAD and also immunoaffinity purified (Thermo Fisher, MA, USA). The pan-UV antibody was described in Lampel et al. (2005). Dry slides were placed in 100% ice-cold acetone bath for 5 min, then washed 3 × 10 min in 0.1 M PBS. Slides were then placed in 0.5% sodium dodecyl sulfate in 0.1 M PBS for 5 min. Each slide was blocked for 30 min at room temperature using 8% (v/v) normal donkey serum and normal goat serum, and 0.3% Triton X-100 in 0.1 M PBS. Slides were incubated with 2:75 affinity-purified rabbit antipan-UV or rabbit antiblue antibody and 1:15 affinity-purified guinea pig antiUV1 antibody in blocking solution overnight at 4 °C. Slides were washed 3 × 10 min in 0.1 M PBS and then incubated with 1:1000 goat antiguinea pig Alexafluor 488 and 1:500 donkey antirabbit Cy3 or Alexafluor 555, in blocking solution for 2 h at room temperature. Slides were washed once more 3 × 10 min in 0.1 M PBS. Slides were stored for imaging by coverslipping with Aqua Poly/Mount (Polysciences, Inc. Cat. # 18606). Slides were viewed with epifluorescence microscopy using a Zeiss Axioskop 2 under a 20× lens. Images were taken using a Zeiss Axiocam HRc and associated Axiovision software, or with a Leica confocal SP700 microscope in the UC Irvine Optical Core Facility. Contrast and brightness were adjusted for clarity using Adobe Photoshop CS4 and Fiji.

For each specimen, we examined hundreds to thousands of fluorescently labeled ommatidia at multiple depths in the retina, and we noted different ommatidial types based on the combinations of UV-expressing R1 and R2 cells. For clarity, all images are presented as a small subset of the retina, where all possible ommatidial combinations can be seen in close proximity. We fluorescently labeled R1 and R2 cells expressing either BRh (blue), UVRh1 (green), or UVRh2 (magenta) (fig. 1*B–L*, supplementary fig. S1*A–N*, Supplementary Material online). We did not distinguish which cell was R1 and which was R2. In double stains that did not label BRh expression, R1 and R2 cells that were not labeled were assumed to be blue opsin expressing cells, according to previous

in situ hybridization and current immunohistochemistry results (fig. 1; Zaccardi et al. 2006). We then classified ommatidial types according to their combination of R1 and R2 cells, and identified retinal mosaics by the combinations of ommatidial types present in each (fig. 1B).

RNA-Sequencing

Total RNA was extracted from 62 individual adult butterfly heads using Trizol (Life Technologies, Grand Island, NY). A NucleoSpin RNA II kit (Macherey-Nagel, Bethlehem, PA) was used to purify 10 μg total RNA per sample. Purified total RNA was quantified using a Qubit 2.0 Fluorometer (Life Technologies, Grand Island, NY). The quality of the RNA samples was checked using an Agilent Bioanalyzer 2100 (Agilent Technologies, Santa Clara, CA). Four micrograms of purified total RNA were used to make cDNA libraries. A TruSeq RNA sample prep kit, set A (Illumina, San Diego, CA) was used to prepare individual cDNA libraries. PCR-enriched individual cDNA libraries were quantified using the Qubit 2.0 Fluorometer and QC checked using the Agilent Bioanalyzer 2100. After being normalized according to their Qubit concentrations, the enriched individual libraries were pooled and then run on a 2% agarose gel. cDNA products ranging from 280 to 340 bp with an average of 310 bp were cut out and purified using a Geneclean III kit (MP Biomedicals, Solon, OH). After being repurified using Agencourt AMPure XP magnetic beads (Beckman Coulter Genomics, Danvers, MA), the cDNA pool was quantified using the Qubit 2.0 Fluorometer, and QC checked using the Agilent Bioanalyzer 2100. The cDNA pool sample was then normalized to 10 nM and run on a HiSeq 2000 (Illumina, San Diego, CA) yielding ~200 million 100 bp paired-end reads per lane.

Cell Counting and Principal Component Analysis

Ommatidia were only counted if images captured more than 100 ommatidia, the tissue was not sheared or folded, and cell bodies were clearly labeled without a high level of background. Images were viewed at full resolution in Adobe Illustrator. The background autofluorescence found in all ommatidia was not removed, so as to see any ommatidia that might be unstained. Ommatidia were not counted if the staining was unclear or the sectioned tissue was of poor quality (e.g., folded). Total ommatidia were counted over as much area as possible for a single high quality section per individual and the percentages of each class of ommatidia were calculated. From these ommatidial classes, we could count the total number of individual R1 and R2 photoreceptor subtypes found in each section. Principal components analysis was performed in R using the prcomp function of the stats package. Ommatidial and cell count averages for each sex and species were used and log transformed for the analysis. The results were plotted using the first two principal components as the *x*- and *y*-axes.

Ancestral State Reconstruction and Character Mapping

Twenty-seven species of *Heliconius* and *E. isabella* were scored for the presence or absence of full-length *UVRh2* transcripts. All species expressed *UVRh1*. Fourteen species representing each of the major *Heliconius* lineages and the outgroup *Eueides isabella* were examined using immunohistochemistry and scored for the presence or absence of the following four traits: female and male UVRh1 and UVRh2 PRCs. Each of these four characters were individually mapped onto the terminal nodes of the species tree from ref (Kozak et al. 2015) in Mesquite (Maddison and Maddison 2011) and ancestral states were then estimated using the maximum likelihood MK1 model with equal likelihood of gains and losses.

Opsin Phylogenies

LWRh, *BRh*, *UVRh1*, and *UVRh2* opsin nucleotide sequences were gathered from GenBank or assembled from 62 newly sequenced individual *Heliconius* and *Eueides* head transcriptomes (representing 21 species). Included in this data set are closely related outgroups from three genera: *Eueides* (*E. isabella*, *E. procula*, *E. aliphera*, *E. lineata*, and *E. vibilia*), *Dione* (*D. juno* and *D. moneta*), and *Agraulis vanillae*. mRNA-Seq data were *de novo* assembled in CLC Genomics and opsin sequences were identified through local database BLAST searches, and then added to the MEGA alignments (Tamura et al. 2011). In cases where fragmented assemblies resulted from this procedure, full-length mRNAs from related individuals were used as a template against which reads from individual libraries were mapped. The read-mapping consensus sequence was then inspected by eye, exported, and included in the nucleotide alignments. The number of nucleotide sites used to estimate each of the opsin phylogenies was as follows: *UVRh* (1137 bp), *BRh* (1143 bp), and *LWRh* (1143 bp). 234 newly sequenced mRNA sequences have been deposited in GenBank under accession numbers MF035495-MF035722, and may also be found in supplementary table S1, Supplementary Material online. Individual sequences were excluded from phylogenetic analysis if low expression levels resulted in large gaps. Newly sequenced and previously reported opsin genes (supplementary table S1, Supplementary Material online, Frentiu et al. 2007b; Pohl et al. 2009; Briscoe et al. 2010; Yuan et al. 2010; Bybee et al. 2012; Martin et al. 2013) were used to construct phylogenies in PhyML using the HKY85 substitution model and branch support was calculated with 1,000 bootstrap replicates using aBayes (Guindon et al. 2010; Anisimova et al. 2011).

RELAX Analysis

We used our *UVRh2* sequences to construct a gene tree using PhyML as described above. We defined all *melpomene*/silvaniform *UVRh2* branches as the test branches (*T*), and all other *UVRh2* and outgroup *UVRh* sequences as the reference branches (*R*), and ran the RELAX hypothesis test in HyPhy (Pond et al. 2005) on the High Performance Computing cluster at UC Irvine. If relaxed selection is present, then the ω distribution in *R* should move closer to neutrality in *T*, that is, $\omega > 1$ in *R* should decrease toward 1 in *T*, whereas $\omega < 1$ in *R* should increase toward 1 in *T* (fig. 4B). RELAX sets the ω distribution of *T* equal to the ω distribution of *R*, raised to the power of *k*, or the relaxation parameter. In the null model

$k = 1$, so the ω distributions of T and R are equal. In the alternative model, k is allowed to vary, so that if $k > 1$ T is under stronger selection relative to R, and if $k < 1$, then T is under relaxed selection compared with R. The models are compared using a likelihood ratio test using a χ^2 distribution to test if the alternative model is a better fit.

Read-Mapping of Opsins

In order to validate the results of the immunohistochemistry and quantify the different levels of *UVRh1* and *UVRh2* transcript expression between major clades and sexes, we selected individual butterflies (males and females) for analysis. Our RNA-Seq reads were quality trimmed using the python script TQSfastq.py (http://genomics-pubs.princeton.edu/prv/resources/scripts/TQSfastq.py) with a quality threshold of 20 and a minimum read length of 30. Reads were paired using a second python script, paired_sequence_match.py (https://bitbucket.org/lance_parsons/paired_sequence_utils). We produced de novo assemblies of the transcriptome for each species using the programs Velvet (default settings and a kmer length of 31) (Zerbino and Birney 2008) and Oases (Schulz et al. 2012). We then used BLAT (Kent 2002) to locate the species-specific *UVRh1* and *UVRh2* opsin genes in our *de novo* transcriptomes utilizing the publically available *H. melpomene* sequences as references (NCBI Accession numbers: GU324678.1 [*UVRh1*] and GU324679.1 [*UVRh2*]). Next, we mapped the forward set of reads for each sample onto its species-specific *UVRh1* and *UVRh2* opsin sequences using the program Stampy (Lunter and Goodson 2011). SAMtools was then used to sort the resulting mapped reads (Li et al. 2009), and htseq-count (http://www-huber.embl.de/users/anders/HTSeq/doc/overview.html) was employed to count the number of unique reads that mapped to each opsin sequence. We calculated the reads per kilobase of transcript per million mapped (RPKM) for each gene in each sample. We also calculated the ratio of the average $\log_2$ *UVRh2* reads over the average $\log_2$ *UVRh1* reads. Lastly, for any species and sex combination in which we had two or more samples, we determined whether there was a significant difference in the expression of *UVRh1* and *UVRh2* using a two-sample *t*-test with equal variances.

Species Phylogeny

Five representative species of the major *Heliconius* clades were included in this analysis; *H. melpomene*, *H. erato*, *H. doris*, *H. sara*, and *H. charithonia*. A de novo assembly of RNA-Seq data was performed and transcriptomic data from each of the five species was mapped back to the assembly using Velvet (Zerbino and Birney 2008) and Oases (Schulz et al. 2012). Contigs were filtered for the presence of sequence data in each of the five species, for contig lengths of >200 bp and for BLAST matches with >90% sequence identity and >100 bp long. In total, 634 loci were obtained and alignments for each locus were produced using Clustal W (Larkin et al. 2007) and variable positions flanking indels were masked by Ns to reduce misalignment error in the data set. The 634 loci from the five representative species were concatenated and a partition annotation file denoting the coordinates of each locus was generated. This partitioned data was run in RAxML (Stamatakis 2006) with rapid bootstrapping (1000 bootstraps) and a maximum likelihood search under the General Time Reversible (GTR) substitution model, with a gamma distribution. The alignment file for the 634 loci was deposited in Dryad under data identifier: doi:10.5061/dryad.1j1f3.

Discriminability Modeling

Models of color vision take into account how receptor signals contribute to chromatic (e.g., color opponent) mechanisms (Kelber et al. 2003). For *H. erato* males, whose yellow color preferences have been tested experimentally (Finkbeiner et al. 2014; Finkbeiner et al. 2017) and shown to prefer 3-OHK yellow models, we calculated discriminabilities for the actual *H. erato* male trichromatic system consisting of UV2, blue and green receptors and a hypothetical *H. erato* male trichromatic system in which UV2 is replaced by UV1. Equations from (Kelber et al. 2003) and (Vorobyev and Osorio 1998) were used to model discriminabilities. This model incorporates a von Kries's transformation, that is, normalization by the illumination spectrum, which models the way in which low-level mechanisms such as photoreceptor adaptation give color constancy (Kelber et al. 2003). The sunny cage illumination spectrum from (Finkbeiner et al. 2017) was used in the model because it corresponds to the illumination used during actual *Heliconius erato* behavioral experiments. For *H. erato* photoreceptor spectral sensitivity curves with λmax values = 355 nm (UV1), 390 nm (UV2), 470 nm (B), and 555 (L) nm from (McCulloch et al. 2016a) were used. Parameters for the butterfly visual models were as follows: Weber fraction = 0.05 (Koshitaka et al. 2008), photoreceptor peak sensitivities, λ_{max} = 355 nm (hypothetical UV1 male only) or 390 nm (actual UV2 male only), 470 and 555 nm, and relative abundances of photoreceptors, V = 0.13, B = 0.2, L = 1 (male) or UV=0.09, V=0.07, B=0.17, L=1 (females) (McCulloch et al. 2016a).

Supplementary Material

Supplementary data are available at *Molecular Biology and Evolution* online.

Author Contributions

K.J.M., P.A., and A.D.B. designed the study. K.J.M, Y.Z., and F.Y. performed experiments. K.J.M., Y.Z., M.L.A., G.S., P.A. and A.D.B. analyzed data. J.L.B. provided specimens. K.J.M. and A.D.B. wrote the paper. All authors read and provided input to the paper.

Acknowledgments

We thank Aide Macias Muñoz for technical assistance with RNA-Seq, Claudia Hernández, Larry Gilbert, and Robert Reed for help with collecting, and Antónia Monteiro, Claude Desplan, Michael Perry, Daniel Osorio, Johannes Spaethe, Martin Streinzer, Anthony Long, and Timothy Bradley for discussions and comments on the manuscript. This work was supported by the Programa de Apoyo a Proyectos de Investigación e Innovación Tecnológica (DGAPA-UNAM IN-

214212 to J.L.); UCMEXUS-CONACYT (CN-13-591 to A.D.B. and J.L.); and the National Science Foundation (IOS-1257627 to A.D.B. and P.A. and IOS-1656260 to A.D.B.). This work was also made possible, in part, through access to the confocal facility of the optical biology shared resource of the cancer center support grant (CA-62203) at the University of California, Irvine. GenBank Accession Nos for opsin sequences are: MF035495–MF035722. Correspondence and requests for materials should be addressed to A.D.B. (abriscoe@uci.edu) and K.J.M. (mccullok@uci.edu).

References

Andersson S, Dobson HE. 2003. Antennal responses to floral scents in the butterfly *Heliconius melpomene*. *J Chem Ecol.* 29:2319–2330.

Anisimova M, Gil M, Dufayard JF, Dessimoz C, Gascuel O. 2011. Survey of branch support methods demonstrates accuracy, power, and robustness of fast likelihood-based approximation schemes. *Syst Biol.* 60:685–699.

Arikawa K. 2003. Spectral organization of the eye of a butterfly, *Papilio*. *J Comp Physiol A Neuroethol Sens Neural Behav Physiol.* 189:791–800.

Arikawa K, Wakakuwa M, Qiu X, Kurasawa M, Stavenga DG. 2005. Sexual dimorphism of short-wavelength photoreceptors in the small white butterfly, *Pieris rapae crucivora*. *J Neurosci.* 25:5935–5942.

Blackiston D, Briscoe AD, Weiss MR. 2011. Color vision and learning in the monarch butterfly, *Danaus plexippus* (Nymphalidae). *J Exp Biol.* 214:509–520.

Bok MJ, Porter ML, Cronin TW. 2015. Ultraviolet filters in stomatopod crustaceans: diversity, ecology and evolution. *J Exp Biol.* 218:2055–2066.

Briscoe AD, Bernard GD, Szeto AS, Nagy LM, White RH. 2003. Not all butterfly eyes are created equal: rhodopsin absorption spectra, molecular identification, and localization of ultraviolet-, blue-, and green-sensitive rhodopsin-encoding mRNAs in the retina of *Vanessa cardui*. *J Comp Neurol.* 458:334–349.

Briscoe AD, Bernard GD. 2005. Eyeshine and spectral tuning of long wavelength-sensitive rhodopsins: no evidence for red-sensitive photoreceptors among five Nymphalini butterfly species. *J Exp Biol.* 208:687–696.

Briscoe AD, Bybee SM, Bernard GD, Yuan F, Sison-Mangus MP, Reed RD, Warren AD, Llorente-Bousquets J, Chiao CC. 2010. Positive selection of a duplicated UV-sensitive visual pigment coincides with wing pigment evolution in *Heliconius* butterflies. *Proc Natl Acad Sci U S A.* 107:3628–3633.

Briscoe AD, Macias-Munoz A, Kozak KM, Walters JR, Yuan F, Jamie GA, Martin SH, Dasmahapatra KK, Ferguson LC, Mallet J, et al. 2013. Female behaviour drives expression and evolution of gustatory receptors in butterflies. *PLoS Genet.* 9:e1003620.

Bybee SM, Yuan F, Ramstetter MD, Llorente-Bousquets J, Reed RD, Osorio D, Briscoe AD. 2012. UV photoreceptors and UV-yellow wing pigments in *Heliconius* butterflies allow a color signal to serve both mimicry and intraspecific communication. *Am Nat.* 179:38–51.

Chen PJ, Arikawa K, Yang EC. 2013. Diversity of the photoreceptors and spectral opponency in the compound eye of the Golden Birdwing, *Troides aeacus formosanus*. *PLoS One* 8:e62240.

Chen PJ, Awata H, Matsushita A, Yang E-C, Arikawa K. 2016. Extreme spectral richness in the eye of the common bluebottle butterfly, *Graphium sarpedon*. *Front Ecol Evol*. 4. doi:10.3389/fevo.2016.00018.

Cook T, Pichaud F, Sonneville R, Papatsenko D, Desplan C. 2003. Distinction between color photoreceptor cell fates is controlled by prospero in *Drosophila*. *Dev Cell* 4:853–864.

Cronin TW, Marshall NJ. 1989. A retina with at least ten spectral types of photoreceptors in a mantis shrimp. *Nature* 339:137–140.

Cronin TW, Bok MJ, Marshall NJ, Caldwell RL. 2014. Filtering and polychromatic vision in mantis shrimps: themes in visible and ultraviolet vision. *Philos Trans R Soc Lond B Biol Sci.* 369:20130032.

Dalton BE, Lu J, Leips J, Cronin TW, Carleton KL. 2015. Variable light environments induce plastic spectral tuning by regional opsin coexpression in the African cichlid fish, *Metriaclima zebra*. *Mol Ecol.* 24:4193–4204.

Dalton BE, de Busserolles F, Marshall NJ, Carleton KL. 2017. Retinal specialization through spatially varying cell densities and opsin coexpression in cichlid fish. *J Exp Biol.* 220:266–277.

Domingos PM, Brown S, Barrio R, Ratnakumar K, Frankfort BJ, Mardon G, Steller H, Mollereau B. 2004. Regulation of R7 and R8 differentiation by the *spalt* genes. *Dev Biol.* 273:121–133.

Estrada C, Jiggins CD. 2008. Interspecific sexual attraction because of convergence in warning colouration: is there a conflict between natural and sexual selection in mimetic species?. *J Evol Biol.* 21:749–760.

Everett A, Tong X, Briscoe AD, Monteiro A. 2012. Phenotypic plasticity in opsin expression in a butterfly compound eye complements sex role reversal. *BMC Evol Biol.* 12:232.

Finkbeiner SD, Briscoe AD, Reed RD. 2014. Warning signals are seductive: relative contributions of color and pattern to predator avoidance and mate attraction in *Heliconius* butterflies. *Evolution* 68:3410–3420.

Finkbeiner SD, Fishman DA, Osorio D, Briscoe AD. 2017. Ultraviolet and yellow reflectance but not fluorescence is important for visual discrimination of conspecifics by *Heliconius erato*. *J Exp Biol.* 220:1267–1276.

Franceschini N, Hardie R, Ribi W, Kirschfeld K. 1981. Sexual dimorphism in a photoreceptor. *Nature* 291:241–244.

Frentiu FD, Bernard GD, Cuevas CI, Sison-Mangus MP, Prudic KL, Briscoe AD. 2007a. Adaptive evolution of color vision as seen through the eyes of butterflies. *Proc Natl Acad Sci U S A.* 104:8634–8640.

Frentiu FD, Bernard GD, Sison-Mangus MP, Brower AV, Briscoe AD. 2007b. Gene duplication is an evolutionary mechanism for expanding spectral diversity in the long-wavelength photopigments of butterflies. *Mol Biol Evol.* 24:2016–2028.

Frentiu FD, Yuan F, Savage WK, Bernard GD, Mullen SP, Briscoe AD. 2015. Opsin clines in butterflies suggest novel roles for insect photopigments. *Mol Biol Evol.* 32:368–379.

Friedrich M, Wood EJ, Wu M. 2011. Developmental evolution of the insect retina: insights from standardized numbering of homologous photoreceptors. *J Exp Zool B Mol Dev Evol.* 316:484–499.

Futahashi R, Kawahara-Miki R, Kinoshita M, Yoshitake K, Yajima S, Arikawa K, Fukatsu T. 2015. Extraordinary diversity of visual opsin genes in dragonflies. *Proc Natl Acad Sci USA.* 112:E1247–E1256.

Guindon S, Dufayard JF, Lefort V, Anisimova M, Hordijk W, Gascuel O. 2010. New algorithms and methods to estimate maximum-likelihood phylogenies: assessing the performance of PhyML 3.0. *Syst Biol.* 59:307–321.

Heliconius Genome Consortium. 2012. Butterfly genome reveals promiscuous exchange of mimicry adaptations among species. *Nature* 487:94–98.

Hofmann CM, Carleton KL. 2009. Gene duplication and differential gene expression play an important role in the diversification of visual pigments in fish. *Integr Comp Biol.* 49:630–643.

Kelber A, Vorobyev M, Osorio D. 2003. Animal colour vision: behavioural tests and physiological concepts. *Biol Rev.* 78:81–118.

Kent WJ. 2002. BLAT: the BLAST-like alignment tool. *Genome Res.* 12:656–664.

Kosakovsky Pond SL, Murrell B, Fourment M, Frost SD, Delport W, Scheffler K. 2011. A random effects branch-site model for detecting episodic diversifying selection. *Mol Biol Evol.* 28:3033–3043.

Koshitaka H, Kinoshita M, Vorobyev M, Arikawa K. 2008. Tetrachromacy in a butterfly that has eight varieties of spectral receptors. *Proc Biol Sci.* 275:947–954.

Kozak KM, Wahlberg N, Neild AF, Dasmahapatra KK, Mallet J, Jiggins CD. 2015. Multilocus species trees show the recent adaptive radiation of the mimetic *Heliconius* butterflies. *Syst Biol.* 64:505–524.

Lampel J, Briscoe AD, Wasserthal LT. 2005. Expression of UV-, blue-, long-wavelength-sensitive opsins and melatonin in extraretinal

photoreceptors of the optic lobes of hawk moths. *Cell Tissue Res.* 321:443–458.
Larkin MA, Blackshields G, Brown NP, Chenna R, McGettigan PA, McWilliam H, Valentin F, Wallace IM, Wilm A, Lopez R, et al. 2007. Clustal W and Clustal X version 2.0. *Bioinformatics* 23:2947–2948.
Li H, Handsaker B, Wysoker A, Fennell T, Ruan J, Homer N, Marth G, Abecasis G, Durbin R, Genome Project Data Processing S. 2009. The sequence alignment/map format and SAMtools. *Bioinformatics* 25:2078–2079.
Lunter G, Goodson M. 2011. Stampy: a statistical algorithm for sensitive and fast mapping of Illumina sequence reads. *Genome Res.* 21:936–939.
Macias-Muñoz A, Smith G, Monteiro A, Briscoe AD. 2016. Transcriptome-wide differential gene expression in *Bicyclus anynana* butterflies: female vision-related genes are more plastic. *Mol Biol Evol.* 33:79–92.
Maddison WP, Maddison DR. 2011. Mesquite: a modular system for evolutionary analysis. Version 2.75. Available from: http://mesquiteproject.org.
Martin A, Papa R, Nadeau NJ, Hill RI, Counterman BA, Halder G, Jiggins CD, Kronforst MR, Long AD, McMillan WO, et al. 2012. Diversification of complex butterfly wing patterns by repeated regulatory evolution of a *Wnt* ligand. *Proc Natl Acad Sci U S A.* 109:12632–12637.
Martin SH, Dasmahapatra KK, Nadeau NJ, Salazar C, Walters JR, Simpson F, Blaxter M, Manica A, Mallet J, Jiggins CD. 2013. Genome-wide evidence for speciation with gene flow in *Heliconius* butterflies. *Genome Res.* 23:1817–1828.
McCulloch KJ, Osorio D, Briscoe AD. 2016a. Sexual dimorphism in the compound eye of *Heliconius erato*: a nymphalid butterfly with at least five spectral classes of photoreceptor. *J Exp Biol.* 219:2377–2387.
McCulloch KJ, Osorio D, Briscoe AD. 2016b. Determination of photoreceptor cell spectral sensitivity in an insect model from in vivo intracellular recordings. *J Vis Exp.* :53829. doi: 10.3791/53829.
Menzel JG, Wunderer H, Stavenga DG. 1991. Functional morphology of the divided compound eye of the honeybee drone (*Apis mellifera*). *Tissue Cell* 23:525–535.
Mikeladze-Dvali T, Wernet MF, Pistillo D, Mazzoni EO, Teleman AA, Chen YW, Cohen S, Desplan C. 2005. The growth regulators *warts/lats* and *melted* interact in a bistable loop to specify opposite fates in *Drosophila* R8 photoreceptors. *Cell* 122:775–787.
Nadeau NJ, Pardo-Diaz C, Whibley A, Supple MA, Saenko SV, Wallbank RWR, Wu GC, Maroja L, Ferguson L, Hanly JJ, et al. 2016. The gene *cortex* controls mimicry and crypsis in butterflies and moths. *Nature* 534:106–110.
O'Quin KE, Schulte JE, Patel Z, Kahn N, Naseer Z, Wang H, Conte MA, Carleton KL. 2012. Evolution of cichlid vision via *trans*-regulatory divergence. *BMC Evol Biol.* 12:251.
Ogawa Y, Awata H, Wakakuwa M, Kinoshita M, Stavenga DG, Arikawa K. 2012. Coexpression of three middle wavelength-absorbing visual pigments in sexually dimorphic photoreceptors of the butterfly *Colias erate*. *J Comp Physiol A Neuroethol Sens Neural Behav Physiol.* 198:857–867.
Ogawa Y, Kinoshita M, Stavenga DG, Arikawa K. 2013. Sex-specific retinal pigmentation results in sexually dimorphic long-wavelength-sensitive photoreceptors in the eastern pale clouded yellow butterfly, *Colias erate*. *J Exp Biol.* 216:1916–1923.
Parry JW, Carleton KL, Spady T, Carboo A, Hunt DM, Bowmaker JK. 2005. Mix and match color vision: tuning spectral sensitivity by differential opsin gene expression in Lake Malawi cichlids. *Curr Biol.* 15:1734–1739.
Perry M, Kinoshita M, Saldi G, Huo L, Arikawa K, Desplan C. 2016. Molecular logic behind the three-way stochastic choices that expand butterfly colour vision. *Nature* 535:280–284.
Pohl N, Sison-Mangus MP, Yee EN, Liswi SW, Briscoe AD. 2009. Impact of duplicate gene copies on phylogenetic analysis and divergence time estimates in butterflies. *BMC Evol Biol.* 9:99.
Pond SL, Frost SD, Muse SV. 2005. HyPhy: hypothesis testing using phylogenies. *Bioinformatics* 21:676–679.
Reed RD, Papa R, Martin A, Hines HM, Counterman BA, Pardo-Diaz C, Jiggins CD, Chamberlain NL, Kronforst MR, Chen R, et al. 2011. *optix* drives the repeated convergent evolution of butterfly wing pattern mimicry. *Science* 333:1137–1141.
Sauman I, Briscoe AD, Zhu H, Shi D, Froy O, Stalleicken J, Yuan Q, Casselman A, Reppert SM. 2005. Connecting the navigational clock to sun compass input in monarch butterfly brain. *Neuron* 46:457–467.
Schulte JE, O'Brien CS, Conte MA, O'Quin KE, Carleton KL. 2014. Interspecific variation in *Rx1* expression controls opsin expression and causes visual system diversity in African cichlid fishes. *Mol Biol Evol.* 31:2297–2308.
Schulz MH, Zerbino DR, Vingron M, Birney E. 2012. Oases: robust *de novo* RNA-seq assembly across the dynamic range of expression levels. *Bioinformatics* 28:1086–1092.
Schulz S, Estrada C, Yildizhan S, Boppre M, Gilbert LE. 2008. An antiaphrodisiac in *Heliconius melpomene* butterflies. *J Chem Ecol.* 34:82–93.
Seehausen O, Terai Y, Magalhaes IS, Carleton KL, Mrosso HD, Miyagi R, van der Sluijs I, Schneider MV, Maan ME, Tachida H, et al. 2008. Speciation through sensory drive in cichlid fish. *Nature* 455:620–626.
Sison-Mangus MP, Bernard GD, Lampel J, Briscoe AD. 2006. Beauty in the eye of the beholder: the two blue opsins of lycaenid butterflies and the opsin gene-driven evolution of sexually dimorphic eyes. *J Exp Biol.* 209:3079–3090.
Smith G, Chen Y-R, Blissard GW, Briscoe AD. 2014. Complete dosage compensation and sex-biased gene expression in the moth *Manduca sexta*. *Genome Biol Evol.* 6:526–537.
Stalleicken J, Labhart T, Mouritsen H. 2006. Physiological characterization of the compound eye in monarch butterflies with focus on the dorsal rim area. *J Comp Physiol A Neuroethol Sens Neural Behav Physiol.* 192:321–331.
Stamatakis A. 2006. RAxML-VI-HPC: maximum likelihood-based phylogenetic analyses with thousands of taxa and mixed models. *Bioinformatics* 22:2688–2690.
Tamura K, Peterson D, Peterson N, Stecher G, Nei M, Kumar S. 2011. MEGA5: molecular evolutionary genetics analysis using maximum likelihood, evolutionary distance, and maximum parsimony methods. *Mol Biol Evol.* 28:2731–2739.
Van Belleghem SM, Rastas P, Papanicolaou A, Martin SH, Arias CF, Supple MA, Hanly JJ, Mallet J, Lewis JJ, Hines HM, et al. 2017. Complex modular architecture around a simple toolkit of wing pattern genes. *Nat Ecol Evol.* 1:0052.
van Schooten B, Jiggins CD, Briscoe AD, Papa R. 2016. Genome-wide analysis of ionotropic receptors provides insight into their evolution in *Heliconius* butterflies. *BMC Genomics* 17:254.
Vorobyev M, Osorio D. 1998. Receptor noise as a determinant of colour thresholds. *Proc Roy Soc B Biol Sci.* 265:351–358.
Wakakuwa M, Kurasawa M, Giurfa M, Arikawa K. 2005. Spectral heterogeneity of honeybee ommatidia. *Naturwissenschaften* 92:464–467.
Wang B, Xiao JH, Bian SN, Niu LM, Murphy RW, Huang DW. 2013. Evolution and expression plasticity of opsin genes in a fig pollinator, *Ceratosolen solmsi*. *PLoS One* 8:e53907.
Wernet MF, Mazzoni EO, Celik A, Duncan DM, Duncan I, Desplan C. 2006. Stochastic *spineless* expression creates the retinal mosaic for colour vision. *Nature* 440:174–180.
Wernet MF, Perry MW, Desplan C. 2015. The evolutionary diversity of insect retinal mosaics: common design principles and emerging molecular logic. *Trends Genet.* 31:316–328.
Wertheim JO, Murrell B, Smith MD, Kosakovsky Pond SL, Scheffler K. 2015. RELAX: detecting relaxed selection in a phylogenetic framework. *Mol Biol Evol.* 32:820–832.
Yuan F, Bernard GD, Le J, Briscoe AD. 2010. Contrasting modes of evolution of the visual pigments in *Heliconius* butterflies. *Mol Biol Evol.* 27:2392–2405.
Zaccardi G, Kelber A, Sison-Mangus MP, Briscoe AD. 2006. Color discrimination in the red range with only one long-wavelength sensitive opsin. *J Exp Biol.* 209:1944–1955.
Zerbino DR, Birney E. 2008. Velvet: algorithms for *de novo* short read assembly using de Bruijn graphs. *Genome Res.* 18:821–829.